Article

Research on Four-Phase Interleaved Step-Up DC/DC Converter for Photovoltaic Energy Storage System

Xiaogang Wu [1,2], Boyang Yu [1], Jiuyu Du [2,*], Wenwen Shi[1]

[1] School of Electrical and Electronic Engineering, Harbin University of Science and Technology, Harbin 150080, Heilongjiang, China; xgwu@hrbust.edu.cn (X.W.); yuboyang_ma17@hrbust.edu.cn (B.Y.); shiwenwen_ma16@hrbust.edu.cn (W.S.)

[2] State Key Laboratory of Automotive Safety and Energy, Tsinghua University, Beijing 100084, China; dujiuyu@tsinghua.edu.cn

* Correspondence: dujiuyu@tsinghua.edu.cn

Received: date; Accepted: date; Published: date

Abstract: Intended for the high voltage gain and wide-range operation of DC/DC converters for photovoltaic energy storage systems, a topology for four-phase interleaved DC/DC converters for photovoltaic power generation is proposed. This topology increases output voltage for output in series, and reduces the input current ripple by paralleling the input. Compared with traditional boost converter topology, the proposed topology reduces the output current and output voltage ripple, reduces the stress of the switching device, and reduces the withstanding voltage of the output capacitor under the premise of ensuring the boost ratio. Experimental results show that the maximum efficiency of the converter reaches 95.37%. Compared with traditional boost converters, the proposed converter offers obvious advantages in efficiency under the conditions that the output voltage and load are variable.

Keywords: DC-DC converter, photovoltaic energy storage system, high voltage gain, high efficiency

1. Introduction

A photovoltaic energy storage system not only solves the problem of uncertainty in solar power generation, but also reduces environmental pollution and solves the problem of shortage of non-renewable resources [1]. The existence of a DC/DC converter solves the problem of power conversion between a photovoltaic power generation system and a DC bus [2]. The output voltage of a single solar panel is generally 18 V or 36 V, and the DC bus voltage is generally 500 V. Therefore, the requirements that such DC/DC converters need to meet are a higher boost ratio, higher efficiency, smaller input current and output voltage ripple, higher power density, wider voltage gain range, and long-term stable operation [3]. Traditional boost converters have difficulty meeting the above requirements because of their own topological characteristics.

In the literature on the topology of DC/DC converters for the optical storage of combined power generation systems, study [4] proposed a new type of DC/DC converter structure for high-frequency transformer integration and high-voltage power distribution. This structure had the advantages of high frequency voltage transformation, high efficiency, and high voltage operation. Study [5] proposed a wide input voltage, high-efficiency non-isolated DC/DC converter that solved the problem of large fluctuation in the input voltage, and had a simple structure, high efficiency, and strong anti-interference ability. Study [6] proposed a novel non-isolated, zero-voltage switching (ZVS), interleaved DC-DC boost converter that recycled energy stored in the inductor by using a coupled inductor and an active clamp circuit. In addition, ZVS conduction of the main switch and clamp switch could be realized. The active clamp circuit suppressed the voltage spike on the main switch, and the voltage of the clamp capacitor increased the boost ratio. Study [7] proposed a new non-isolated stepper DC/DC converter in which the voltage stress of the switch and diode of the converter was small. The active-passive inductor unit was used to expand the topology. The parallel charging and series discharging of inductors gave the converter higher voltage gain. Study [8] proposed a diode-rectified quasi-Z source (BTL-DRqZ) DC/DC converter with a low voltage stress that achieved zero current effect when turned on or turned off". It showed a wide range of voltage gain while using synchronous rectification technology to reduce the losses of the quasi-Z source circuit. Study [9] proposed a new DC/DC converter that did not use electrolytic capacitors, which reduced the resonance between the parasitic inductance and the parasitic capacitance of the switching tube. The coupling inductance showed small leakage inductance and high conversion efficiency. Study [10] proposed a new type of current-fed dual-active bridge DC/DC converter that could be applied to photovoltaic energy storage systems. The converter realized a soft switching function and had the advantages of wide input voltage range, high boost ratio, and small input current ripple. Study [11] proposed a novel and efficient DC/DC converter for photovoltaic energy storage systems. The converter had no switching loss and realized zero-current switching and zero-voltage switching with a single switch, which is highly efficient. Study [12] proposed a high-performance quasi-Z source DC/DC converter that could be used in photovoltaic systems. The converter guaranteed a 400 V ripple-free output within a range of 6 times the input voltage (10–60 V), which is highly efficient. In [13], a non-isolated high-power DC/DC converter with a voltage multiplier was proposed. In order to obtain a higher voltage gain and efficiency, the converter used three interleaved coupling inductors and three voltage multipliers, each of which consisted of a secondary winding of the coupling inductor, two diodes, and two charging capacitors. Study [14] proposed a novel zero-current switching current-fed half-bridge DC/DC converter that solved the problem of turn-off voltage spikes with no additional active clamp or snubber circuit. This converter had low cost and high conversion efficiency. Study [15] proposed a high efficiency DC/DC converter for photovoltaic systems. The converter consisted of an active resonant clamp circuit and a harmonic voltage multiplier. The active clamp circuit limited the voltage stress and enabled the switching device to achieve the effect of soft switching. A resonant voltage multiplier was used on the reverse side of the transformer to eliminate the reverse recovery of the output diode. Study [16] proposed a soft-switching high-order DC/DC converter. The converter used a dual-coupled inductor and a shared input current structure. It had high voltage gain and high efficiency. The coupling inductor used a small magnetized inductor to reduce the current ripple at the input end. Study [17] proposed a single-switch boost DC/DC converter with a diode-capacitor module. The converter used a power switch and a small amount of inductance and capacitance. It achieved a wide range of voltage gain and high efficiency with a simple topology. In this structure, two capacitors were charged in parallel and discharged in series. In [18], a high gain, non-isolated soft-switching DC/DC converter was proposed. The auxiliary switch of the converter was connected with the output port to act as an active clamp circuit, thus realizing zero-current switching and improving the efficiency of the converter.

In summary, the research on DC/DC converter topology has mainly focused on improving the efficiency, stability, and reliability of the converter while completing the high boost ratio function. In the practical application of photovoltaic energy storage systems, we should also consider reducing device stress, output current, and output voltage ripple to improve the reliability of the converter [19]. In this paper, a four-phase interleaved DC/DC converter is proposed for a photovoltaic energy storage system to solve the problem of power conversion between the photovoltaic power generation system and the DC bus. The converter has the characteristics of high boost ratio, low output voltage ripple, low power device stress, and high efficiency.

2. Analysis of topology of photovoltaic energy storage system and DC/DC converter

The structure of the photovoltaic energy storage system presented in this paper is shown in Figure 1. The photovoltaic array is connected to the DC bus through a four-phase interleaved boost converter to realize the functions of boost, voltage stabilization, and maximum power point tracking. In order to simplify the analysis, the load determines resistance, and the switching of resistance is used to simulate the power fluctuation in the load.

Preprints (www.preprints.org) | NOT PEER-REVIEWED | Posted: 17 April 2019 doi:10.20944/preprints201904.0202.v1

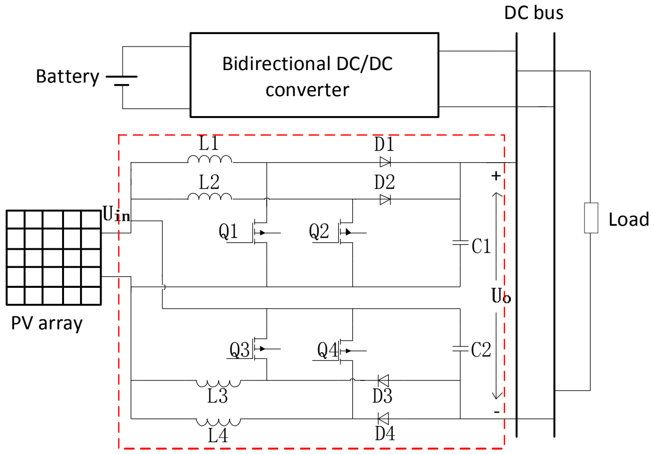

Figure 1 Photovoltaic energy storage system

The four-phase interleaved boost converter consists of four power switches: Q1, Q2, Q3, Q4; four energy storage inductors: L1, L2, L3, L4; two diodes: D1, D2; and two output capacitors: C1 and C2, as shown in Figure 2. The topology uses a four-phase interleaving technique. The phase of each phase circuit differs by 90 electrical degrees, which increases the output current frequency by a factor of four and reduces the ripple after superposition. Moreover, the converter has a relatively high boost, which meets the basic requirements of a DC/DC converter for a photovoltaic energy storage system.

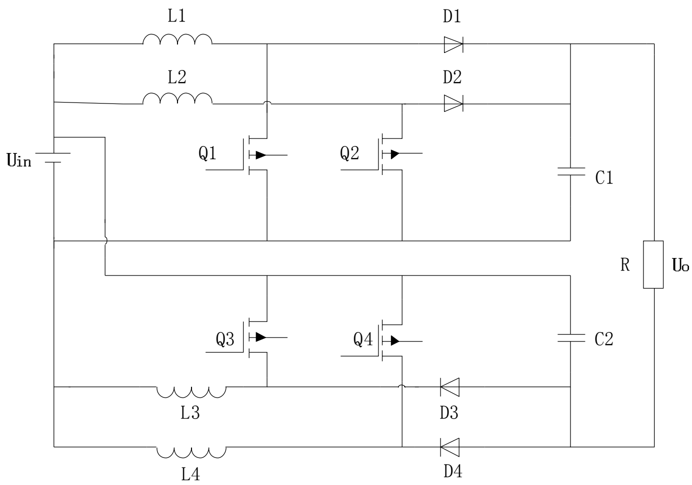

Figure 2 Four-phase interleaved step-up DC/DC converter

Assuming that each device in Figure 2 is an ideal component, the parameters of each inductor and the switch are the same, and the four switches correspond to different states when turned on (ON) or turned off (OFF).

Taking the switch tube Q1 as an example for analysis, when the switch tube is in the ON state, the circuit operation mode is as shown in Figure 3.

Preprints (www.preprints.org) | NOT PEER-REVIEWED | Posted: 17 April 2019 doi:10.20944/preprints201904.0202.v1

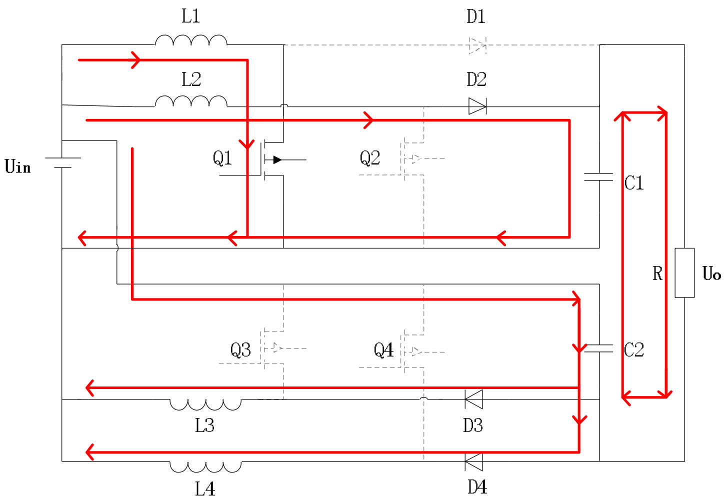

Figure 3 Working mode when Q1 is turned on

There are five loops in the circuit. The power source, U_{in}, the switch tube, Q1, and the inductor, L1, form a loop for charging inductor L1. The other three inductors, L2, L3, and L4, form three loops with power source U_{in} and the two capacitors C1 and C2 through the three diodes D2, D3, and D4 of the branch. The last loop is formed by power source U_{in}, capacitors C1 and C2, and the load, R. Capacitors C1 and C2 supply energy to the load according to the relationship shown in equation (1).

$$U_{\text{in}} + U_{\text{o}} = U_{C1} + U_{C2} \tag{1}$$

Ignoring the turn-on voltage drop of the MOSFET, we assume the direction of the voltage and current is the reference current direction. In one cycle, T_S, the on-time of the switching transistor Q1 is $D \times T_S$, where D is the duty ratio of the Pulse Width Modulation (PWM) wave. At this time, if the current of inductor L1 is I_L, the energy absorbed by inductor L1 is as shown in equation (2).

$$W_L = U_{\text{in}} \times I_L \times D \times T_S \tag{2}$$

When the switch Q1 is in the OFF state, the circuit working mode is as shown in Figure 4.

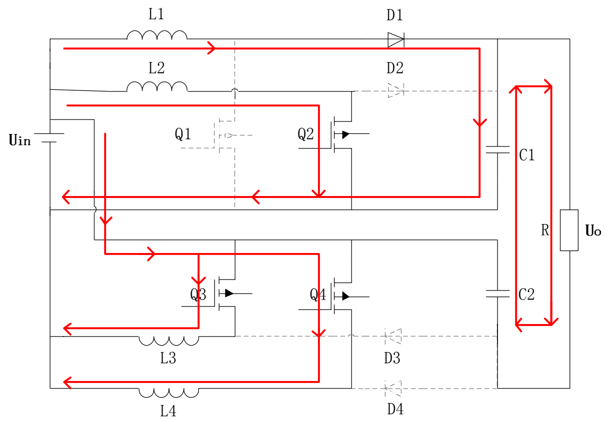

Figure 4 Working mode when Q1 is turned off

The input power U_{in} and inductor L1 are connected in series to charge capacitor C1 through diode D1, forming the first circuit. The other three inductors, L2, L3, and L4, form three loops with the power supply through the three switching tubes Q2, Q3, and Q4, respectively. Capacitors C1 and C2 provide energy to the load to form the last loop, and their relationship is shown by equation (1). At this time, the energy released by inductor L_1 is as shown in equation (3).

Preprints (www.preprints.org) | NOT PEER-REVIEWED | Posted: 17 April 2019 doi:10.20944/preprints201904.0202.v1

$$W_L' = (U-E)\times I_L \times (1-D)\times T_S \tag{3}$$

The energy absorbed and released by inductors L2, L3, and L4 controlled by the other three switches, Q2, Q3, and Q4, is the same as that of inductor L1. According to the law of energy conservation, the energy absorbed and released by the inductor in a PWM cycle is equal to:

$$W_L = W_L' \tag{4}$$

After simplification, the relationship between input voltage U_{in} and voltage U_{C1} on capacitor C1 in the four-phase staggered boost DC/DC converter can be obtained under ideal conditions:

$$U_{C1} = \frac{1}{1-D} U_{in} \tag{5}$$

Substituting equation (1) into equation (5), the voltage gain of the boost converter can be obtained as:

$$G_d = \frac{1+D}{1-D} \tag{6}$$

Figure 5 shows the relationship between the boost ratio of the four-phase interleaved step-up DC/DC converter and the MOSFET duty cycle.

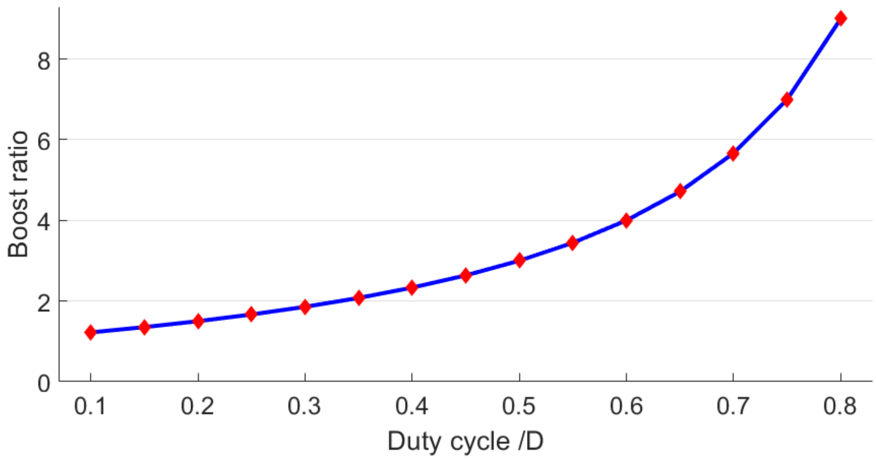

Figure 5 Relation between boost ratio of converter and duty cycle of MOSFET

3. Working mode of four-phase interleaved DC/DC converter

In order to further analyze the working mode of the four-phase interleaved step-up DC/DC converter, this paper establishes the state equation. The effects of inductor current ripple and capacitor voltage fluctuations on the circuit are ignored when establishing the equation of state. Figure 6 is the waveform of the four-phase staggered boost DC/DC converter during the working process, in which the phase difference between the driving signals of the four power switches is 90 electrical degrees.

Preprints (www.preprints.org) | NOT PEER-REVIEWED | Posted: 17 April 2019 doi:10.20944/preprints201904.0202.v1

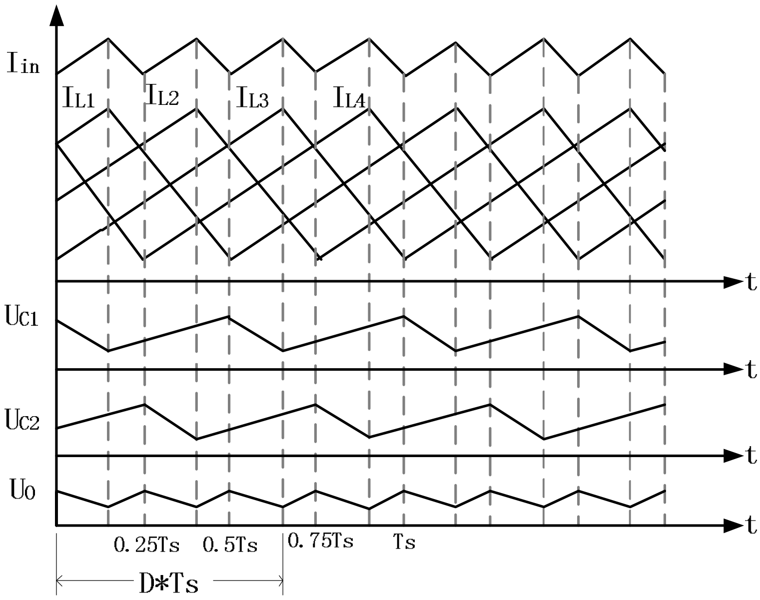

Figure 6 Working waveform of four-phase interleaved boost converter

When switch Q1 is turned on, diode D1 is in the reverse turned-off state. The voltage of inductor L1 is the input voltage, U_{in}; the inductor current increases linearly, and the voltage of capacitor C1 decreases. The change in current in this state is expressed as:

$$L_1 \frac{dI_{L1}}{dt} = U_{in} \tag{7}$$

The voltage change of capacitor C1 is expressed as:

$$C_1 \frac{dU_{C1}}{dt} = -\frac{U_O}{R} \tag{8}$$

We substitute equation (1) into equation (8) to obtain:

$$C_1 \frac{dU_{C1}}{dt} = -\frac{2U_{C1}}{R} + \frac{U_{in}}{R} \tag{9}$$

From equation (7) and equation (9), we obtain the equation of state for this stage as follows:

$$\begin{bmatrix} \frac{dI_{L1}}{dt} \\ \frac{dU_{C1}}{dt} \end{bmatrix} = \begin{bmatrix} 0 & 0 \\ 0 & -\frac{2}{RC_1} \end{bmatrix} \cdot \begin{bmatrix} I_{L1} \\ U_{C1} \end{bmatrix} + \begin{bmatrix} \frac{1}{L_1} \\ \frac{1}{RC_1} \end{bmatrix} \cdot U_{in} \tag{10}$$

When switch Q1 is turned off, diode D1 is turned on, and inductor L1 is connected in series with input power source U_{in} to supply power to the load. The current, I_{L1}, of inductor L1 decreases linearly, and the voltage, U_{C1}, of capacitor C1 rises due to energy supplementation. The change in the inductance current at this stage should be expressed as follows:

$$L_1 \frac{dI_{L1}}{dt} = U_{in} - U_{C1} \tag{11}$$

The voltage equation of capacitor C1 is as follows:

$$C_1\frac{dU_{C1}}{dt}=2I_{L1}-\frac{U_O}{R} \tag{12}$$

Substituting equation (1) into equation (12), we obtain:

$$C_1\frac{dU_{C1}}{dt}=2I_{L1}-\frac{2U_{C1}}{R}+\frac{U_{in}}{R} \tag{13}$$

From equation (11) and equation (13), we obtain the equation of state for this stage as follows:

$$\begin{bmatrix}\frac{dI_{L1}}{dt}\\ \frac{dU_{C1}}{dt}\end{bmatrix}=\begin{bmatrix}0 & -\frac{1}{L_1}\\ \frac{2}{C_1} & -\frac{2}{RC_1}\end{bmatrix}\cdot\begin{bmatrix}I_{L1}\\ U_{C1}\end{bmatrix}+\begin{bmatrix}\frac{1}{L_1}\\ \frac{1}{RC_1}\end{bmatrix}\cdot U_{in} \tag{14}$$

In order to evaluate the performance of the four-phase staggered DC/DC converter, this study compares it with the boost converter commonly used in photovoltaic energy storage systems [20]. First, the boost ratio of the boost circuit is 1/1-D, and the output capacitor is subjected to the output voltage U_o. The four-phase interleaved boost converter has a boost ratio of 1+D/1-D, and its output capacitor is subjected to $(U_{in}+U_o)/2$, which facilitates component selection and cost reduction. Second, the inductor current of the traditional boost circuit is the input current I_{in}. In this study, four-phase interleaving technology is adopted to reduce the inductor current of each phase circuit to $(I_{in}+I_o)/4$, the frequency of the inductor current becomes four times that of the inductor current of traditional boost converter, and the ripple after superposition will be correspondingly reduced.

For boost circuits, the slopes of the inductance current rise (angle u) and fall (angle d) as follows:

$$\left(\frac{dI_L}{dt}\right)_u=\frac{U_{in}}{L} \tag{15}$$

$$\left(\frac{dI_L}{dt}\right)_d=\frac{U_{in}-U_C}{L} \tag{16}$$

Therefore, if f_{sw} is the switching frequency, the inductor current ripple of the boost circuit is:

$$\Delta I_L=\frac{D\cdot U_{in}}{L\cdot f_{sw}} \tag{17}$$

For a four-phase interleaved boost converter, the total current ripple is:

$$\Delta I_4=\begin{cases}\frac{1-4D}{1-D}\Delta I_L\ , & 0\le \mathrm{D}\le 0.25;\\ \frac{-0.5+3D-4D^2}{D(1-D)}\Delta I_L\ , & 0.25<D\le 0.5;\\ \frac{-1.5+5D-4D^2}{D(1-D)}\Delta I_L\ , & 0.5<D\le 0.75;\\ \frac{4D-3}{D}\Delta I_L\ , & 0.75<D\le 1.\end{cases} \tag{18}$$

4. Experimental result verification

In order to verify the effectiveness of the proposed four-phase interleaved DC/DC boost converter in photovoltaic energy storage systems, an experimental prototype as shown in Figure 6 was designed. The experimental prototype design indicators were: an input voltage of 20 V, a rated output voltage of 100 V, a rated output power of 100 W, and a switching frequency of 20 kHz.

Preprints (www.preprints.org) | NOT PEER-REVIEWED | Posted: 17 April 2019 doi:10.20944/preprints201904.0202.v1

According to the above indexes, the corresponding parameters of the selected device are determined.

The calculation formulas of inductors L1, L2, L3, and L4 are:

$$L_1 = L_2 = L_3 = L_4 = \frac{U_{\text{in}} \times D}{2 \times \Delta I_{IN} \times f} \quad (19)$$

ΔI_{IN} is the input current fluctuation and it takes the value of 20% of the average current. Substituting the experimental prototype design indicator into equation (19), after calculation, L1=L2=L3=L4=0.35 mH.

The calculation formula of capacitors C1 and C2 is:

$$C_1 = C_2 = \frac{I_{out} \times D}{\Delta U \times f} \quad (20)$$

ΔU is the output voltage fluctuation and it takes the value of 1% of the output voltage. Substituting the experimental prototype design indicator into equation (20), after calculation, two electrolytic capacitors with a capacitance of 47 μF and a withstanding voltage of 400 V were selected.

After analysis and calculation, the voltage of the switch tube was found to be $(U_{in}-U_o)/2=60$ V. Considering a two- to three-fold margin, a model IRF640N power MOSFET was selected as the switching transistor. The maximum on-current was 18 A and the maximum withstanding voltage was 200 V. The reverse voltage drop of the diode was $U_{C1}-U_{in}$ and the output current was 1 A. Considering a two- to three-fold margin, a model DFE10I600PM diode was selected. This model can withstand the maximum reverse voltage of 600 V, the conduction current of 10 A, and the maximum forward voltage drop of 1.5 A.

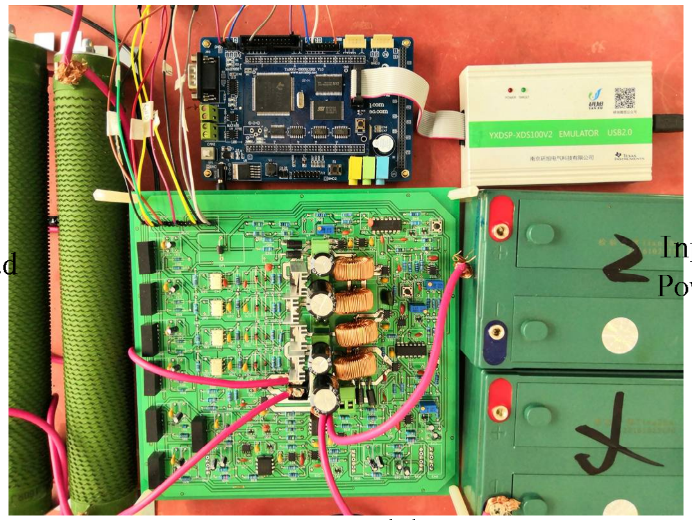

Figure 6 Designed power module prototype

In order to verify the feasibility of the proposed four-phase interleaved boost converter in photovoltaic energy storage system, this study compares it with the boost converter commonly used in current PV energy storage systems.

To compare boost ratios between the four-phase interleaved boost converter and the traditional boost converter, the actual boost ratios of the four-phase interleaved boost converter and the traditional boost converter were tested. The driving signal of the former switching tube is four PWM waves, and each phase differs by 90 electrical degrees. The comparison curve of the two boost ratios at the same duty ratio after the test is shown in Figure 7.

Preprints (www.preprints.org) | NOT PEER-REVIEWED | Posted: 17 April 2019 doi:10.20944/preprints201904.0202.v1

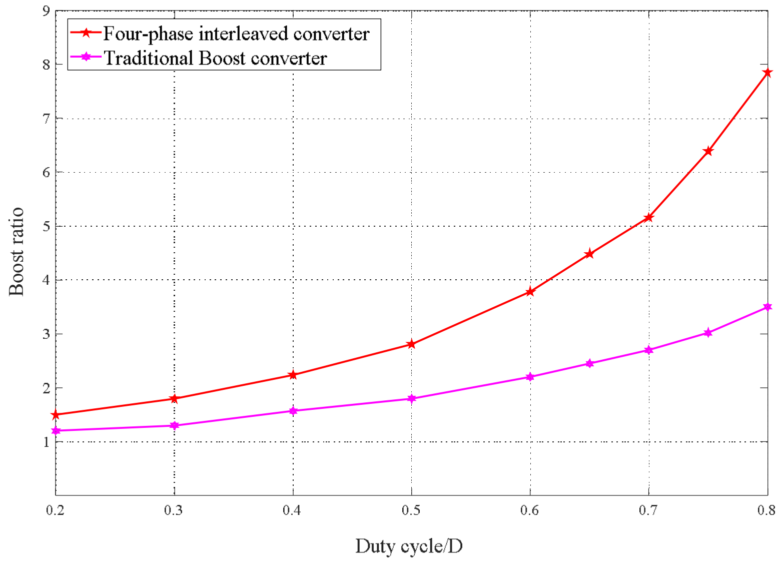

Figure 7 Comparison curve of actual boost ratio of two converters

As can be seen from Figure 7, when the duty cycle is approximately 0.2, the actual boost ratio of the Boost converter is 1.25 times. The actual boost ratio of the four-phase interleaved DC/DC converter is 1.5 times, which is 1.2 times that of the traditional boost converter. With the increase in duty ratio, the gap between the four-phase staggered DC/DC converter and the traditional boost converter becomes increasingly obvious. When the duty ratio is 0.8, the boost ratio of the four-phase interleaved DC/DC converter is 2.24 times that of the traditional boost converter. Figure 8 shows that the increasing degree of boost ratio of the four-phase interleaved DC/DC converter is greater than the traditional boost converter in the duty cycle range from 0.2 to 0.8.

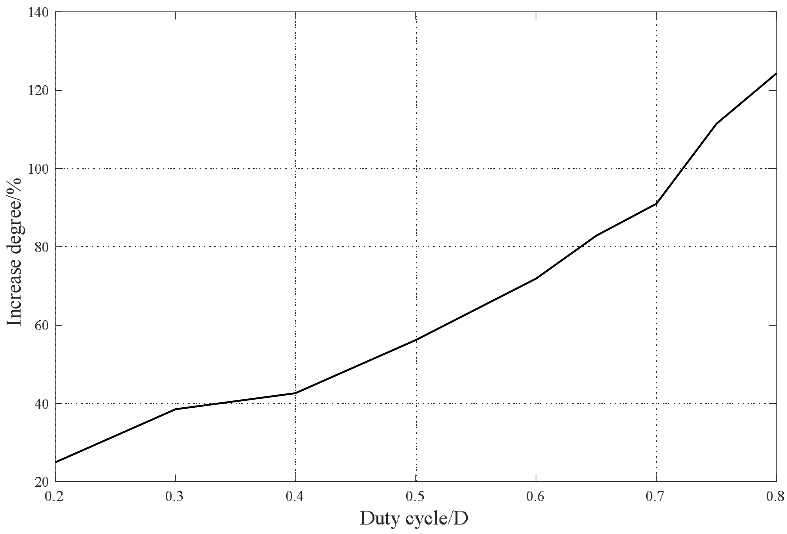

Figure 8 Increasing degree of boost ratio of the four-phase interleaved DC/DC converter is greater than the traditional boost converter

As shown in Figure 8, when duty cycle D equals 0.8, the maximum increase degree is 124.3%. When duty cycle D equals 0.2, the minimum increase is 25%. Compared with the traditional boost converter, the four-phase interleaved DC/DC converter has a wider range and higher gain than the traditional boost converter ; therefore, it is more suitable for the application of photovoltaic power output in photovoltaic energy storage system.

Preprints (www.preprints.org) | NOT PEER-REVIEWED | Posted: 17 April 2019 doi:10.20944/preprints201904.0202.v1

To compare the output voltage ripple of the four-phase interleaved DC/DC converter and the traditional boost converter, we set the input voltage to 6 V and the output voltage to 20 V in a closed loop test of the PID control algorithm. The output voltage waveforms of the two converters were obtained as shown in Figure 9. As can be seen from Figure 9, the ripple coefficient of the output voltage of the traditional boost converter is 0.015, while that of the four-phase interleaved DC/DC converter is 0.0075. Compared with the traditional boost converter, output voltage ripple of the four-phase interleaved DC/DC converter is superior.

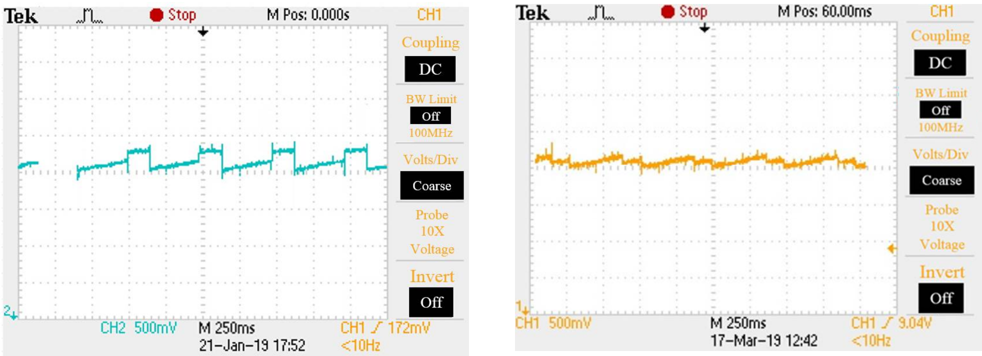

a) Traditional boost converter b) Four-phase interleaved DC/DC converter

Figure 8 Output voltage ripple of two converters

In order to further demonstrate the advantages of the four-phase interleaved DC/DC converter in photovoltaic energy storage system applications, the input voltage was set to 24 V and the load was set to 100. The efficiency of the four-phase interleaved DC/DC converter and the traditional boost converter were tested separately. Because the traditional boost converter has a duty ratio of 0.2 to 0.8, the output voltage varies from 30 V to 85 V. The output voltage range of the four-phase interleaved DC/DC converter varies from 30 V to 120 V. The efficiency comparison of the two DC/DC converters is shown in Figure 10.

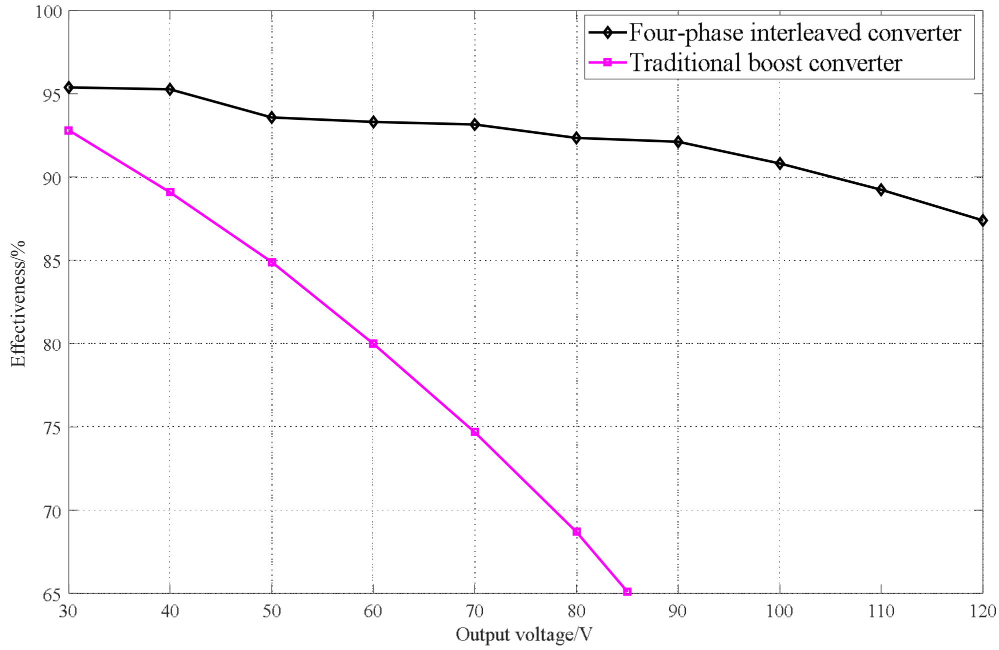

Figure 10 Comparison of efficiency between two types of boost converters

Preprints (www.preprints.org) | NOT PEER-REVIEWED | Posted: 17 April 2019 doi:10.20944/preprints201904.0202.v1

It can be seen from Figure 10 that when the output load is constant, the loss in the boost converter is related to the inductor current and duty cycle when the switching frequency is determined. The higher the output voltage, the larger the inductor current and duty cycle, resulting in higher inductance losses and on-state losses of the switching device, which reduces system efficiency. Therefore, the four-phase interleaved DC/DC converter has an efficiency of 95.37% at an output voltage of 30 V, and the lowest efficiency is 87.38% at an output voltage is 120 V. The boost converter has an efficiency of 92.8% at an output voltage of 30 V, and an efficiency of 65.1% at an output voltage of 85 V. In addition, regardless of the output voltage, the efficiency of the four-phase interleaved DC/DC converter is higher than that of the boost converter. Moreover, the higher the output voltage, the more obvious the efficiency advantage.

In this paper, the efficiency of the four-phase interleaved DC/DC converter and boost converter is tested under the condition of constant output voltage and different loads. Setting the output voltage to 50 V, and beginning with a load of 50 Ω, the efficiency of the two converters was tested every 5 Ω until the load reached 100 Ω. The comparison results are shown in Figure 11.

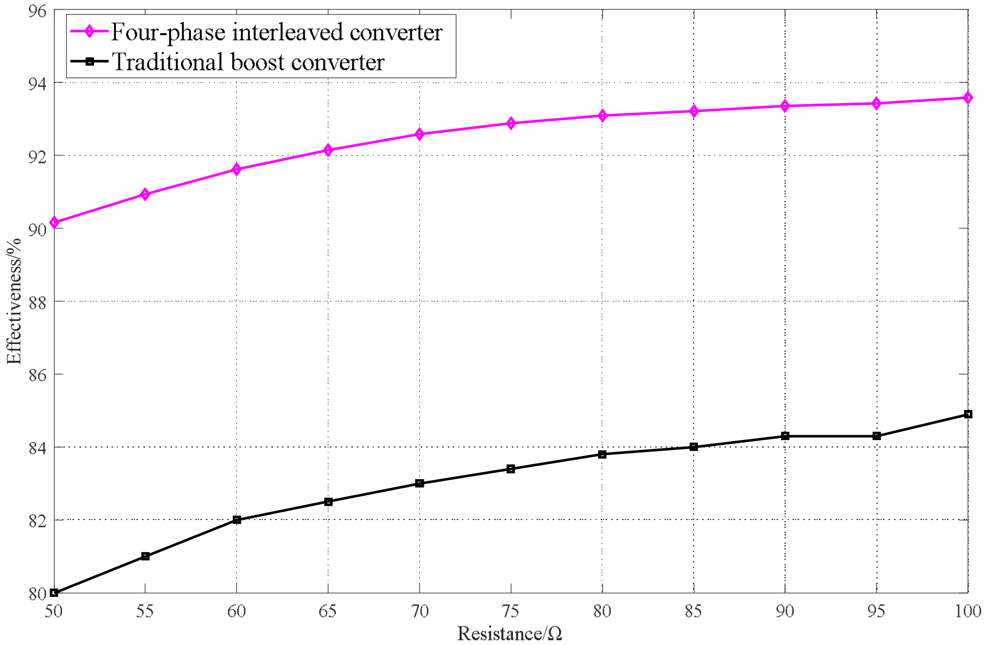

Figure 10 Efficiency corresponding to different loads when the output voltage is 50 V

As can be seen from Figure 11, when the output voltage is 50 V, increasing the load reduces the inductance loss and the switch-on loss, because the circuit loss is related to the on-current and the on-time, and the greater the duty cycle and on-current, the greater the on-state loss of the switching transistor. Therefore, the efficiency of quad-phase interleaved DC/DC converters and boost converters increases by varying degrees with increases in the load. When the load is 50 Ω, the lowest efficiency is 90.16%, and when the load is 50 Ω, the highest efficiency is 93.59%. The traditional boost circuit has a maximum efficiency of 84.9% and a minimum efficiency of 80%. The efficiency of the four-phase interleaving DC/DC converter is much higher than that of the boost converter under the same load.

5. Conclusion

Considering the requirements of wide gain range, high boost ratio, and small output voltage ripple in a DC/DC converter for photovoltaic energy storage system, a four-phase interleaved DC/DC converter was proposed for a photovoltaic energy storage system. Based on the analysis of the working principle of DC/DC converters, an experimental prototype was designed. A

 doi:10.20944/preprints201904.0202.v1

comparative study was carried out with the boost converter commonly used in photovoltaic energy storage systems.

1. Considering the boost ratio, switching tube stress, and output capacitor with standing voltage, the four-phase interleaved DC/DC converter showed obvious advantages over the boost circuit. The four-phase interleaved DC/DC converter adopted interleaving technology, which greatly reduced the output current ripple and output voltage.
2. Comparison of the integrated boost ratio, output voltage ripple, and system efficiency showed that four-phase staggered DC/DC converters are more efficient than traditional boost converters regardless of output voltage and load, and when the load is constant, the larger the output voltage, the more obvious the advantage of the four-phase interleaved DC/DC converter in terms of efficiency.

Acknowledgments: This work was sponsored through the National Key Technologies R&D Program of MOST (2018YFB0105403); University Nursing Program for Young Scholars with Creative Talent in Heilongjiang Province (UNPYSCT-2016164); State Key Laboratory of Automotive Safety and Energy under Project No. KF1826.

References

[1] Sharma P , Agarwal V . Exact Maximum Power Point Tracking of Grid-Connected Partially Shaded PV Source Using Current Compensation Concept[J]. IEEE Transactions on Power Electronics, 2014, 29(9):4684-4692.
[2] Denholm P , Margolis R , Mai T , et al. Bright Future: Solar Power as a Major Contributor to the U.S. Grid[J]. Power & Energy Magazine IEEE, 2013, 11(2):22-32.
[3] Yang C , Qin L , Xie S , et al. Stable operating area of photovoltaic cells feeding DC–DC converter in output voltage regulation mode[J]. IET Renewable Power Generation, 2015, 9(8):970-981.
[4] Moonem M A , Krishnaswami H . Control and Configuration of Three-Level Dual-Active Bridge DC-DC Converter as a Front-end Interface for Photovoltaic System[J]. IEEE Applied Power Electronics Conference and Exposition，2014：3017-3020.
[5] Aguillon-Garcia J , BaNUelos-Sanchez P . High-Efficiency DC-DC Converter for Large Input-Voltage Fluctuations in Solar Applications[J]. Chinese Journal of Electronics, 2015, 24(3):502-507.
[6] Talebi S., Adib E., Delshad M. A high gain soft switching interleaved DC-DC converter[J]. IEICE Transactions on Electronics, 2018,906-915.
[7] Babaei E , Mashinchi Maheri H , Sabahi M , et al. Extendable Non-isolated High Gain DC-DC Converter Based on Active-Passive Inductor Cells[J]. IEEE Transactions on Industrial Electronics, 2018:9478-9487.
[8] Zhang Y , Shi J , Zhou L , et al. Wide Input-Voltage Range Boost Three-Level DC–DC Converter With Quasi-Z Source for Fuel Cell Vehicles[J]. IEEE Transactions on Power Electronics, 2017, 32(9):6728-6738.
[9] Freitas A A A , Antunes F L M , Daher S , et al. High-voltage gain dc–dc boost converter with coupled inductors for photovoltaic systems[J]. IET Power Electronics, 2015, 8(10):1885-1892.
[10] Shi Y , Li R , Xue Y , et al. Optimized Operation of Current-fed Dual Active Bridge DC-DC Converter for PV Applications[J]. IEEE Transactions on Industrial Electronics, 2015, 62(11):6986-6995.
[11] Fathabadi, Hassan. Novel high efficiency DC/DC boost converter for using in photovoltaic systems[J]. Solar Energy, 2016, 125:22-31.
[12] Vinnikov D , Chub A , Liivik E , et al. High-Performance Quasi-Z-Source Series Resonant DC–DC Converter for Photovoltaic Module-Level Power Electronics Applications[J]. IEEE Transactions on Power Electronics,2017, 32(5):3634-3650.

Preprints (www.preprints.org) | NOT PEER-REVIEWED | Posted: 17 April 2019 doi:10.20944/preprints201904.0202.v1

[13] Revathi B S , Prabhakar M . Nonisolated High Gain DC-DC Converter Topologies for PV Applications - A Comprehensive Review[J]. Renewable and Sustainable Energy Reviews, 2016, 66:920-933.

[14] Prasanna U R , Rathore A K , Mazumder S K . Novel Zero-Current-Switching Current-Fed Half-Bridge Isolated DC/DC Converter for Fuel-Cell-Based Applications[J]. IEEE Transactions on Industry Applications, 2013, 49(4):1658-1668.

[15] Cha W J , Kwon J M , Kwon B H . Highly efficient step-up dc–dc converter for photovoltaic micro-inverter[J]. Solar Energy, 2016, 135:14-21.

[16] Liu Y , Abu-Rub H , Ge B . Front-End Isolated Quasi-Z-Source DC–DC Converter Modules in Series for High-Power Photovoltaic Systems—Part I: Configuration, Operation, and Evaluation[J]. IEEE Transactions on Industrial Electronics, 2016, 64(1):347-358.

[17] Zhang Y , Zhou L , Sumner M , et al. Single-Switch, Wide Voltage-Gain Range, Boost DC–DC Converter for Fuel Cell Vehicles[J]. IEEE Transactions on Vehicular Technology, 2018, 67(1):134-145.

[18] Sathyan S , Suryawanshi H , Singh B , et al. ZVS-ZCS High Voltage Gain Integrated Boost Converter For DC Microgrid[J]. IEEE Transactions on Industrial Electronics, 2016:6898-6908.

[19] El Khateb A H , Rahim N A , Selvaraj J , et al. DC-to-DC Converter With Low Input Current Ripple for Maximum Photovoltaic Power Extraction[J]. IEEE Transactions on Industrial Electronics, 2015, 62(4):2246-2256.

[20] Saravanan S , Babu N R . Performance analysis of boost & Cuk converter in MPPT based PV system[C].16 July 2015 International Conference on Circuit. IEEE, 2015.